alies (Fig. 3, a and b). The structure of the high-velocity core is nonunique. Possible models range from a diameter of 50 km and a seismic velocity 10 percent higher than that of the normal mantle to 85 km and 4 percent, respectively. The rapid decrease in the observed travel time for P_{200} between the azimuths 32° and 34° (Fig. 3a) is well modeled by the ray that travels around the anomaly. Hence the diameter of the low-velocity collar at a depth of 200 km is fairly well constrained at 250 ± 30 km. The velocity contrast between the collar and the normal mantle must be as large as 2 percent in order to delay sufficiently the ray passing through the collar. However, an upper bound on the velocity contrast cannot be determined. At 400 km, the rapid decrease in travel time between 32° and 34° is absent. The smoother anomaly is modeled by the ray that travels through the collar. The respective diameter is at least 300 km, and the velocity contrast appears to be less than 2 percent. For both models the center of the structure is shifted approximately 40 km northwest from the center of the caldera.

The simple structure described above is inadequate to completely model the anomaly. Rays passing through the center of the anomaly are advanced and rays passing through the collar or around the anomaly are delayed with respect to the model. We expect that a more complete model that we are developing, employing radial velocity gradients within the plume, will remove this defect. Finally, the structure does not appear to be entirely symmetrical. The southeast shoulder of both the P_{200} and the P_{400} anomalies (Fig. 3, a and b) appears to be somewhat broader than the northwest shoulder. This asymmetry implies a differing collar radius between the northwest and southeast sides of the structure.

Anderson (*10*) has recently discussed a chemical plume model that essentially predicts the observed travel times. In his model, conduits through the mantle contain residuals from the differentiation of the primitive earth. The chemical plume is enriched with CaO, Al_2O_3, TiO_2, and the refractory elements including U and Th. The $CaO\text{-}Al_2O_3\text{-}TiO_2$ assemblage and the refractory elements are expected to have higher seismic velocities than normal ferromagnesian silicates. Thermal perturbations from the decay of the radioactive refractory elements would depress the seismic velocities in the mantle surrounding the plume. The resulting structure would be a cylindrical body with a relatively high-velocity core and a low-velocity collar. The velocity structure and the vertical extent of this feature is consistent with a chemical mantle plume beneath the Yellowstone caldera. The asthenosphere above the chemical plume is more extensively molten than elsewhere, thereby giving lower velocities. The thermal plume hypothesis gives the same result in this region but predicts quite different results at depths greater than about 200 km. Within the lithosphere both the chemical plume and the thermal plume hypotheses give the same result. Melting is expected to be extensive, seismic velocities are reduced, and attenuation is increased.

DAVID M. HADLEY
GORDON S. STEWART
JOHN E. EBEL

Seismological Laboratory,
California Institute of Technology,
Pasadena 91125

References and Notes

1. G. P. Eaton, R. L. Christiansen, H. M. Iyer, A. M. Pitt, D. R. Mabey, H. R. Blank, Jr., I. Zietz, M. E. Gettings, *Science* **188**, 787 (1975).
2. A. M. Pitt, *Eos Trans. Am. Geophys. Union* **56**, 1190 (1974).
3. W. J. Morgan, *Geol. Soc. Am. Mem.* **132**, 7 (1972); V. Mathews and C. E. Anderson, *Nature (London)* **243**, 158 (1972).
4. H. M. Iyer, personal communication.
5. ______, *Nature (London)* **253**, 425 (1975).
6. R. A. Wiggins and D. V. Helmberger, *J. Geophys. Res.* **78**, 1870 (1973).
7. Gravity Map Series of the Dominion Observatory (Department of Energy, Mines, and Resources, Ottawa, Ont., Canada, 1968).
8. F. Press and S. Biehler, *J. Geophys. Res.* **69**, 2979 (1964).
9. Tectonic Map of Canada 1251A (Geological Survey of Canada, Ottawa, Ont., 1968).
10. D. L. Anderson, *Geol. Soc. Am. Bull.* **86**, 1593 (1975)
11. We thank R. S. Hart for assistance in the preparation for the fieldwork and H. M. Iyer for encouragement and useful discussions on the current Yellowstone P delay project. This research was supported by U.S. Geological Survey contract 14-08-0001-15250. Contribution No. 2733, Division of Geological and Planetary Sciences, California Institute of Technology.

29 March 1976

Snowfall Observations from Natural-Draft Cooling Tower Plumes

Abstract. *During the winter of 1975–1976, snowfall from the plumes of large natural-draft cooling towers of power plants has been observed. Snow accumulations up to 2.5 centimeters have been found on the ground at extended distances from the cooling towers, and visibility has been restricted to less than 1600 meters in the tower plume near ground level.*

Five American Electric Power System (AEP) power plants in Kentucky, Ohio, and West Virginia are equipped with natural-draft cooling towers (Fig. 1). In this area there are several rivers capable of supplying condensing water for power plants of the size that were being installed in the early 1950's. In the last 20 years, however, the increase in the size of the power plants combined with concern over the potential effects on the rivers has led to a shift from direct, once-through systems to cooling towers, as shown in Table 1.

In view of the prospect of cooling towers capable of discharging 1.25×10^9 kg-cal per hour, studies of plume rise and persistence under various meteorological conditions were undertaken by the American Electric Power Service Corporation and Smith-Singer Meteorologists, Inc., at the Muskingum River and Big Sandy power plants during the fall of 1968. From 1968 through 1970 these studies consisted of visual observations and photographs of the plumes taken from the ground; temperature, humidity, and wind measurements were also recorded. By the third year of this exploratory study, we became convinced that airborne observations were necessary to study plume behavior accurately and to establish firm relationships with meteorological conditions. During the last three winters (1973 through 1976) measurements of ambient temperature and humidity were recorded from light aircraft. Each test also included visual and photographic records of the geometry of the visible plumes, and wind data were obtained from aircraft drift measurements.

Table 1. Growth of AEP generating capacity.

Period	Additional capacity installed during period (Mw)	Percentage of new capacity using cooling towers
1950–1954	1980	0
1955–1959	1920	23
1960–1964	1970	25
1965–1969	2510	53
1970–1974	5570	100

Up to March 1975, no significant environmental effects had been found at any of the natural-draft towers studied. Data from the 1973–1975 flight tests (*1*) indicated that no precipitation or fog was induced at ground level by these towers. On the contrary, all of the visible plumes, a few of which traveled 25 km or more from the plants, remained at least 450 m above ground.

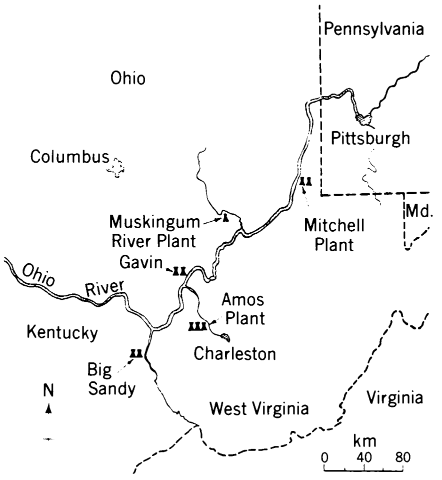

Fig. 1. Location of AEP natural-draft cooling towers.

During the two winters of 1973–1975 there were no flights with temperatures in the test region as low as −12°C. Since the moisture capacity of the atmosphere decreases to less than 2 g/m³ below this temperature, we modified the test program so that flights were scheduled only when temperatures of −12°C or less were forecast. With such a small moisture deficit and such a large release of water vapor, very persistent plumes and even precipitation seemed likely.

During the winter of 1975–1976 the first significant environmental effect was observed. Large natural-draft towers produced plumes persisting as far as 70 km in which the supercooled water droplets changed to ice crystals and produced light snowfall. Measurable accumulations of snow were observed on the ground. The falling snow restricted visibility to less than 1600 m close to the ground. From December 1975 through March 1976, this conversion of liquid droplets to ice crystals was observed ten times at several power plants in the test area. One of these incidents is described below.

During a period of clear weather on 18 January 1976, from 0755 to 1111 E.S.T., a flight test was conducted in the vicinity of the Amos plant, located 25 km northwest of Charleston, West Virginia. This coal-fired plant has three hyperbolic cooling towers serving three generators totaling 2900 Mw. The weather was cold and clear with temperatures of −12°C near the surface, decreasing to −20°C at 1600 m above ground, as shown in Fig. 2. The plumes from the three cooling towers merged and rose to form a typical liquid droplet cloud between 900 and 1600 m. The plumes mixed with the smokestack effluent at 400 m. The rise of the cooling tower plume stopped at the base of an elevated temperature inversion, also at 1600 m. The change from supercooled droplets to ice crystals began at 5 km and was complete 11 km downwind of the towers. This ice crystal cloud persisted aloft to a distance downwind of 43 km. Snow began descending from the base of the plume when the conversion from droplets to ice crystals started, and it first reached the ground at 13 km. Snowfall on the ground also continued to at least 43 km. The maximum accumulation of snow (very light fluffy snow) was 2.5 cm (Fig. 3).

The ground measurements shown outside of the plume shadow (Fig. 3) indicate that the plume trajectory had changed from the initial conditions before our test started. The visibility in the clear air was greater than 15 km, but it was restricted to approximately 1600 m in the snow near the ground level, as it would be in a natural snowfall.

It was not possible to measure the cooling tower performance characteristics and the exit parameters in this program. However, the cooling tower manufacturers have stated that each of the two smaller towers at this plant has a maximum capacity of circulating water of 940,000 liters per minute and the largest tower 2,270,000 liters per minute. Approximately 1 to 2 percent of this circulating water is evaporated at full load at any given ambient conditions. The average loads on each of the smaller towers were 300 and 750 Mw, respectively, out of a possible 800 Mw each; the third tower operated at 1300 Mw, full load, throughout the test.

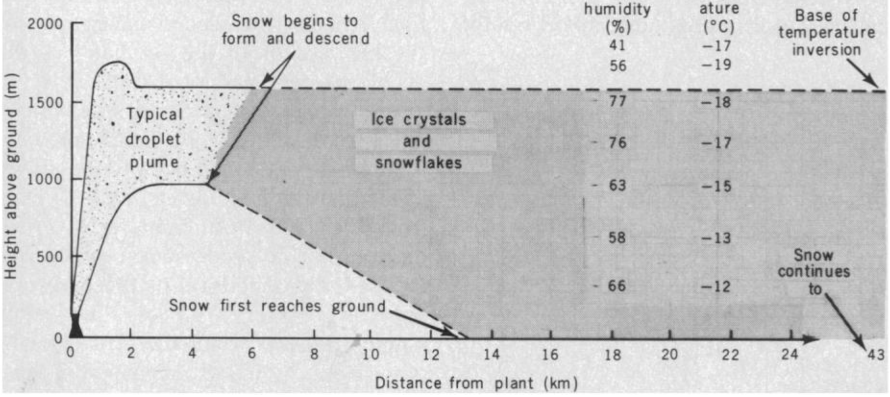

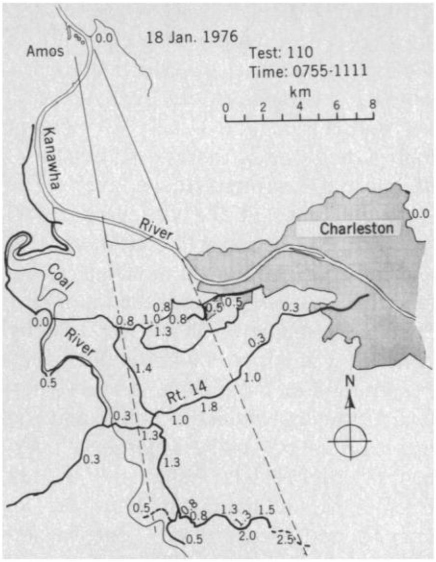

Fig. 3. Measured snow depths (in centimeters) under the visible ice crystal plume from the cooling tower.

In some of the tests at Amos and at other plants, natural clouds were present and snow or snow showers came from them. This natural snow occurred before, during, or after the observations of snow from the cooling tower plumes. Snow was observed from the tower plumes, however, when it was not falling from natural clouds. Moreover, the conversion of the tower plumes from liquid drops to ice crystals sometimes induced a similar change in the natural clouds, creating an obvious "hole" in an otherwise unbroken cloud deck.

We cannot specify precisely the conditions required for induced snow. Observations to date have indicated that induced snow has been associated with low temperatures and with plumes diffusing in relatively stable conditions. The key parameters are air temperatures of −12°C or less and relatively stable diffusion conditions at plume height. The rate of water vapor emission from the towers must be critical also, since this is the source of the additional water vapor.

If the flights in this study have shown this effect on ten occasions in one winter, one wonders why artificially induced snowfall has not been reported before. One important reason may be that most natural-draft cooling towers are located in moderate to warm climates. In our test area, for example, there were no very cold flight days in the winters of 1973–1974 and 1974–1975. Second, snowfall from the plumes seems to reach the ground at considerable distances from the towers (a minimum distance of 8 km in our tests). In hilly terrain it is difficult to identify the cooling towers as the source, and a ground observer would probably assume that the snow was natural. Third, during the 3-year study of all of the AEP power plants with natural-draft towers and seven plants without cooling towers, no smoke plume alone was observed to produce snow or rain when it combined or merged with a natural cloud deck. Finally, the artificial snowfall often occurs when the atmosphere is cloudy and snow would be expected. In our tests, natural snow often coincided with tower-induced snow or occurred soon afterward.

However, the observations made during the winter of 1975–1976 are not unique. A similar snowfall was observed at Oak Ridge, Tennessee, in 1960 (*2*). The water vapor released from clusters of mechanical draft towers at the gaseous diffusion plant at Oak Ridge approximated that from a large power plant, and the weather conditions were similar to those which induced snow in our observations. Agee (*3*) has also described the artificial inducement of snowfall, but the incident he described appears to have been caused by a seeding effect of particles in supercooled fog. In Hanna and Gifford's recent comprehensive review of the possible meteorological effects of energy parks (*4*), there is no mention of snowfall.

It is too early to assess the environmental importance of the induced snowfall. With power plants in the size range and area studied, the effects seem likely to be minor. Occasional very small additions to natural snow and slight restrictions of visibility are all that one would anticipate. The effects of possible artificial snow must be carefully considered, however, when several large plants are to be clustered together, especially in cold climates.

MARK L. KRAMER
DAVID E. SEYMOUR
MAYNARD E. SMITH
Smith-Singer Meteorologists, Inc., Amityville, New York 11701
ROBERT W. REEVES
THEODORE T. FRANKENBERG
American Electric Power Service Corporation, Canton, Ohio 44701

References

1. M. L. Kramer, M. E. Smith, M. J. Butler, D. E. Seymour, T. T. Frankenberg, *J. Air Pollut. Control Assoc.* **26**, 582 (1976); P. T. Brennan, D. E. Seymour, M. J. Butler, M. E. Smith, T. T. Frankenberg, *Atmos. Environ.* **10**, 425 (1976).
2. W. M. Culkowski, *Mon. Weather Rev.* **194**, 194 (1962).
3. A. M. Agee, *Bull. Am. Meteorol. Soc.* **52**, 557 (1971).
4. S. R. Hanna and F. A. Gifford, *ibid.* **56**, 1069 (1975).

18 March 1976; revised 21 May 1976

Entropy Estimates for Some Silicates at 298°K from Molar Volumes

Abstract. *Third law entropies for silicates of Be, Mg, Ca, Zn, Na, and K containing the same anion group, for example, SiO_4 or SiO_3 or $AlSi_3O_8$, are found to be linearly related to their molar volumes. The relationship between the molar volume and the entropy of silicates of Fe and Mn, atoms with unfilled* d *electron subshells, is different from that of other silicates. The linear correlations yield a useful method of estimating the entropies of ortho-, meta-, and framework silicates (feldspars and feldspathoids). The estimated entropies of pyrope and almandine at 298°K are 47.47 and 68.13 gibbs per mole, respectively.*

In calculations of phase equilibria, in cases where the entropies of silicates are not known the sum of the entropies of the constituent oxides can be substituted (*1, 2*). For many silicates, however, there is a significant difference between the two values. My purpose in this report is to explore the relationship between the entropy and the molar volume of silicates and to find if one can estimate entropy closely by using an empirical entropy-volume relationship. Such estimated entropies may be useful if they are closer to the experimentally determined entropies than those obtained by the oxide summation method.

Table 1 shows the data on experimentally determined entropies and molar vol-

Table 1. Molar volumes and experimental and estimated entropies of anhydrous silicates.

Silicate	Formula	n	Experimental S (gibbs/mole)	V (cm³/mole)	Calculated S (gibbs/mole)	$S_{exp}-S_{calc}$ (gibbs/mole)	$S_{exp}-S_{oxides}$ (gibbs/mole)
Estimated for orthosilicates from Eq. 1, $\sigma = 0.047$ (excluding γ-Ca_2SiO_4)							
Phenacite	Be_2SiO_4	1	15.37	37.19	15.23	0.14	−1.25
Larnite	β-Ca_2SiO_4	1	30.50	51.60	30.17	0.33	1.62
Ca-olivine	γ-Ca_2SiO_4	1	28.80	59.11	37.95	−9.15	−0.08
Grossularite	$Ca_3Al_2Si_3O_{12}$	1/3	57.70	125.3	59.94	−2.25	−12.63
Merwinite	$Ca_3MgSi_2O_8$	1/2	60.50	104.40	61.58	−1.530	−4.54
Forsterite	Mg_2SiO_4	1	22.75	43.79	22.08	0.67	−.01
Willemite	Zn_2SiO_4	1	31.40	52.42	31.02	0.38	0.66
Estimated for metasilicates from Eq. 3, $\sigma = 0.027$							
Wollastonite	$CaSiO_3$	1	19.60	39.93	20.57	−0.97	0.22
Pseudo-wollastonite	$CaSiO_3$	1	20.90	40.08	20.65	0.25	1.08
Ca-Al pyroxene	$CaAlAlSiO_6$	1/2	34.60	63.50	32.24	2.36	3.04
Diopside	$CaMgSi_2O_6$	1/2	34.20	66.09	33.66	0.54	−1.50
Enstatite	$MgSiO_3$	1	16.22	31.47	15.97	0.25	−0.10
Jadeite	$NaAlSi_2O_6$	1/2	31.90	60.47	30.56	1.346	−2.94
Estimated for feldspars and feldspathoids from Eq. 5, $\sigma = 0.014$							
Microcline	$KAlSi_3O_8$	4/15	52.47	108.72	52.44	0.03	5.49
Sanidine	$KAlSi_3O_8$	4/15	56.94	109.05	57.05*	0.11	5.52*
Kaliophilite	$KAlSiO_4$	2/7	31.85	59.89	31.93	−0.08	4.63
Leucite	$KAlSi_2O_6$	3/11	44.05	88.39	43.94	0.11	6.95
Low albite	$NaAlSi_3O_8$	4/15	50.20	100.07	48.90	1.30	5.48
High albite	$NaAlSi_3O_8$	4/15	54.67	100.43	53.52*	1.15	5.48*
Nepheline	$NaAlSiO_4$	2/7	29.72	54.16	29.59	0.13	4.76

*Includes a configurational entropy of disorder of 4.47 gibbs/mole.

Table 2. Molar volumes and experimental and estimated entropies of hydrous silicates. Values are calculated from Eq. 6, where $\sigma = 0.017$.

Silicate	Formula	n	Experimental S (gibbs/mole)	V (cm³/mole)	Calculated S (gibbs/mole)	$S_{exp}-S_{calc}$ (gibbs/mole)	$S_{exp}-S_{oxides}$ (gibbs/mole
Paragonite	$NaAl_3Si_3O_{10}(OH)_2$	4/15	67.61	132.10	67.68	−0.07	0.03
Muscovite	$KAl_3Si_3O_{10}(OH)_2$	4/15	69.00	140.71	71.42	−2.42	0.80
Phlogopite	$KMg_3AlSi_3O_{10}(OH)_2$	4/15	76.40	149.91	75.42	0.98	−0.58
Kaolinite	$Al_2Si_2O_5(OH)_4$	1/2	48.53	99.52	48.72	0.19	−4.77
Tremolite	$Ca_2Mg_5Si_8O_{22}(OH)_2$	1/8	131.19	272.92	140.52	−9.34	−9.73
Chrysotile	$Mg_3Si_2O_5(OH)_4$	1/2	52.9	108.50	52.62	0.28	−7.54
Anthophyllite	$Mg_7Si_8O_{22}(OH)_4$	1/8	133.62	264.47	136.86	−3.23	−11.86
F-phlogopite	$KMg_3AlSi_3O_{10}F_2$	4/15	75.90	146.37	74.44	1.46	
Talc	$Mg_3Si_4O_{10}(OH)_2$	1/4	62.34	136.25	70.17	−7.83	−7.18